SEPSIS

The lung is a host defense niche for immediate neutrophil-mediated vascular protection

Bryan G. Yipp,[1,2]* Jung Hwan Kim,[1,2] Ronald Lima,[2,3] Lori D. Zbytnuik,[2,3] Björn Petri,[2,4,5] Nick Swanlund,[2,3] May Ho,[2,5] Vivian G. Szeto,[2,3] Tamar Tak,[6,7] Leo Koenderman,[6,7] Peter Pickkers,[8] Anton T. J. Tool,[9] Taco W. Kuijpers,[9] Timo K. van den Berg,[9,10] Mark R. Looney,[11] Matthew F. Krummel,[12] Paul Kubes[1,2,3,4,5]*

Bloodstream infection is a hallmark of sepsis, a medically emergent condition requiring rapid treatment. However, up-regulation of host defense proteins through Toll-like receptors (TLRs) and nuclear factor κB requires hours after endotoxin detection. Using confocal pulmonary intravital microscopy, we identified that the lung provides a TLR4–Myd88 (myeloid differentiation primary response gene 88)–dependent and abl tyrosine kinase–dependent niche for immediate CD11b-dependent neutrophil responses to endotoxin and Gram-negative bloodstream pathogens. In an in vivo model of bacteremia, neutrophils crawled to and rapidly phagocytosed *Escherichia coli* sequestered to the lung endothelium. Therefore, the lung capillaries provide a vascular defensive niche whereby endothelium and neutrophils cooperate for immediate detection and capture of disseminating pathogens.

INTRODUCTION

Sepsis is a deleterious host response to an infection that continues to have an unacceptably high mortality (*1*). Of particular concern is that sepsis with bacteremia, or bloodstream infection, has even worse outcomes in humans (*2*). Bloodstream infections are common both in the community (*3*–*5*) and in the hospital (*6*–*9*). *Escherichia coli* is a major overall causative organism found in community-acquired and hospital-acquired bloodstream infections (*3*, *10*). Alarmingly, Gram-negative bacteria are rapidly developing resistance to broad-spectrum antibiotics and, in some circumstances, have become pan-antibiotic–resistant (*11*, *12*). It is now recognized that sepsis is a medical emergency, similar to heart attacks and strokes, whereby every hour of untreated infection markedly decreases the likelihood of patient survival (*13*). Likewise, the innate immune system must provide immediate protection when pathogens enter the bloodstream until the administration of effective antibiotics.

Lipopolysaccharide (LPS) is the major pathogen-associated molecular pattern of Gram-negative bacteria that binds and stimulates Toll-like receptor 4 (TLR4) (*14*). The signaling pathway is extremely well established and includes the activation of myeloid differentiation primary response gene 88 (Myd88) and interleukin-1 receptor–associated kinase, leading to nuclear factor κB translocation to the nucleus, and subsequent transcription and translation of various pro-inflammatory molecules (*15*–*17*). Macrophage begin to synthesize tumor necrosis factor–α (TNF-α) and numerous chemokines, whereas endothelium begins to synthesize E-selectin, intercellular adhesion molecule–1 (ICAM-1), vascular cell adhesion molecule–1, and additional chemokines in an attempt to recruit the main effector cell of innate immunity, namely, the neutrophil (*18*). Neutrophils do not require protein synthesis to perform phagocytosis, oxidant production, degranulation, or neutrophil extracellular trap (NET) release when reacting to pathogens (*19*). Each of these effector functions occurs in seconds after bacteria stimulation and has been attributed to opsonization and rapid production of proinflammatory complement fragments (*20*). LPS, by contrast, classically requires hours for effector function to be fully elicited through transcription and translation. Contrary to this classical view, but for the most part ignored, is the observation that LPS can induce increases in neutrophil cell surface adhesion molecules and binding in minutes (*21*, *22*). The biological relevance of this rapid nontranscriptional response to host defense in vivo is limited.

Conventionally, the capture of free-flowing particles and circulating pathogens is attributed to stationary resident mononuclear cells within the liver and spleen (*23*–*25*). This resident cellular defense system does not require active pursuit or tracking of the pathogen but absolutely requires that the bug remain in the free flow circulation. The liver is home to resident intravascular macrophages called Kupffer cells, which catch free-flowing bacteria via the complement receptor immunoglobulin (CRIg) as they filter through the sinusoids (*26*–*28*). Despite the clear role of resident macrophages in clearing blood-borne pathogens, the major risk factor for acquiring a bloodstream infection is neutropenia (*29*). In addition, the best prognostic factor in bacteremic cancer patients is the recovery of neutrophil counts (*30*). Both humans and mice do not have pulmonary intravascular macrophages (*21*, *22*); however, pathogens can sequester within the massive surface area of the capillary network, potentially evading removal (*26*). Therefore, it is unclear how the host detects and removes bloodstream pathogens within this macrophage-free vascular labyrinth.

[1]Department of Critical Care, Cumming School of Medicine, University of Calgary, Calgary, Alberta, Canada. [2]Calvin, Phoebe and Joan Snyder Institute for Chronic Diseases, Cumming School of Medicine, University of Calgary, Calgary, Alberta, Canada. [3]Department of Physiology and Pharmacology, Cumming School of Medicine, University of Calgary, Calgary, Alberta, Canada. [4]Mouse Phenomics Resource Laboratory, Snyder Institute for Chronic Diseases, Cumming School of Medicine, University of Calgary, Calgary, Alberta, Canada. [5]Department of Microbiology, Immunology and Infectious Diseases, Cumming School of Medicine, University of Calgary, Calgary, Alberta, Canada. [6]Department of Respiratory Medicine, University Medical Center Utrecht, Utrecht, Netherlands. [7]Emma Children's Hospital, Academic Medical Center, University of Amsterdam, Amsterdam, Netherlands. [8]Department of Intensive Care, Radboud University Nijmegen Medical Centre, Nijmegen, Netherlands. [9]Department of Blood Cell Research, Sanquin Research, and Landsteiner Laboratory, Amsterdam, Netherlands. [10]Department of Molecular Cell Biology and Immunology, VU Medical Center, Amsterdam, Netherlands. [11]Departments of Medicine and Laboratory Medicine, University of California, San Francisco, 513 Parnassus Avenue, HSW512, CA 94143–0511, USA. [12]Department of Pathology, University of California, San Francisco, 513 Parnassus Avenue, HSW512, San Francisco, CA 94143–0511, USA.
*Corresponding author. Email: bgyipp@ucalgary.ca (B.G.Y.); pkubes@ucalgary.ca (P.K.)

The prototypical neutrophil recruitment cascade is a multistep process requiring the endothelium to express molecules (selectins) to slow circulating leukocytes (tethering), followed by vascular rolling and firm adhesion (selectins and integrins) (*31*). Last, leukocytes transmigrate the endothelium in a process termed emigration (*32*). However, this canonical recruitment paradigm may not be true for the lung. The capillary vessels, distinct from larger venules, do not require known molecules involved in rolling, such as the selectins, during inflammation (*33*–*35*). Additionally, although integrins can mediate firm adhesion in lung capillaries, the prevailing understanding is that neutrophils lose cellular deformability and become physically stuck within the small vessels and subsequently emigrate into the alveolus (*36*–*38*). It remains unclear whether physically stuck neutrophils provide any biological function other than emigrating into the lung tissue. Emigration in the lung is a distinct process mediated by both CD11/CD18-dependent and CD11/CD18-independent processes contingent on the initial stimulant (*39*–*41*). A previous report demonstrated that, at baseline, a substantial number of extravascular neutrophils inhabited the lung and that, after bacterial stimulation, vascular neutrophils were rapidly arrested in the microvasculature and the resident neutrophils crawled throughout the extravascular space (interstitial and alveolus), yet intravascular crawling was not reported (*42*). The existence of resident extravascular tissue neutrophils in the lung remains controversial and not consistently supported (*43*, *44*). Despite extensive research to delineate molecules required during the neutrophil recruitment cascade leading to tissue emigration, intravascular neutrophil behaviors and functions remain unexplored.

Using pulmonary intravital microscopy, we have found that vascular neutrophils immediately become alerted to the presence of endotoxin or bloodstream infection through TLR4 and Myd88 signaling. After intravenous endotoxin challenge, neutrophils sequestered within the capillaries but not larger venules, polarized, and crawled throughout the endothelium in a CD11b-dependent process. Lung-sequestered bacteria were removed from circulation by the capillary neutrophils. Therefore, we have found a host defense system involving pulmonary capillary circulation and neutrophils that eliminates bloodstream pathogens that are no longer in free-flowing circulation and, thus, not amenable to capture by resident macrophages.

RESULTS

Neutrophils rapidly up-regulate the expression of CD11b after LPS exposure

Nontranscriptional alterations in neutrophil behavior after endotoxin exposure are reported, yet the mechanisms and biological consequences remain less defined (*22*, *38*, *45*). Under untreated conditions, neutrophils, defined by flow cytometry as Ly6G$^+$ (fig. S1), expressed both CD11b and L-selectin. Mouse neutrophils treated with either LPS (5 μg/ml) or a strong chemical proinflammatory stimulus, *N*-formyl-Met-Leu-Phe (fMLP; 1 μM positive control), revealed substantial up-regulation of cell surface CD11b (Fig. 1A) and decrease in L-selectin within minutes, thus replicating previous reports (Fig. 1B) (*21*). As a positive control, the CD11b expression increased with fMLP and L-selectin shed within 4 min of stimulation. LPS-treated neutrophils increased expression of CD11b and shed L-selectin at the 15-min time point, suggesting some delay compared with the fMLP pathway. This effect continued into the 30-min time point. CD11b was assessed in permeabilized cells, and the total CD11b was unaffected, suggesting shuttling of protein from internal granules to the surface (fig. S2). As shown later, these events led to rapid phenotypic changes in neutrophil behavior in vivo and could not be affected by transcription and translational inhibitors.

To confirm that modulation of CD11b occurs in vivo in humans, healthy volunteers received intravenous highly purified LPS (2 ng/kg), and blood was drawn over time to assess neutrophil numbers and how they coincided with CD11b$^+$ expression on neutrophils (Fig. 1, C and D). After 30 min of LPS, the number of circulating neutrophils dropped by 50%, and simultaneously, there was evidence of an increase in CD11b expression. This drop in neutrophil counts and increase of CD11b persisted for at least 90 min. Therefore, human peripheral neutrophil counts dropped as CD11b increased, analogous to our findings later in mice, where neutrophils increased CD11b after LPS and accumulated in the lung. It was impossible to examine the lung vasculature in humans; however, primary human pulmonary endothelium was cultured to confluence, and LPS-stimulated (15 min) human neutrophils, or control-untreated cells, were assayed within a flow chamber to mimic a surrogate lung microvasculature. Neutrophil adhesion on lung endothelium occurred at baseline without stimulation, a phenomenon we have not observed previously using dermal human microvascular cells (*46*). Conventionally, investigations have pretreated human umbilical cord endothelial cells for a minimum of 4 hours before leukocyte adhesion assays to allow time for the synthesis of adhesion molecules such as E-selectin and ICAM-1 (*47*, *48*). However, adhesion was significantly increased after 15 min of LPS stimulation of human neutrophils independent of endothelial pretreatment (Fig. 1E). The parallel plate flow chamber provides a physical space between the endothelium and chamber that is much larger than a capillary dimension; thus, the LPS-treated neutrophils cannot become physically stuck or lodged in this assay, suggesting a different mechanism of rapid adhesion compared with cytoskeleton stiffening (*38*). Collectively, these data support the concept that LPS induces a rapid neutrophil response in humans in vitro and in vivo, leading to modulation of cell surface adhesion molecules. Although rapid changes in integrins and selectins on the surface of neutrophils have been demonstrated, the biological significance and underlying mechanism in vivo that contribute to host defense remain uncertain (*21*). To understand the biology of these observations, we moved to mouse models and imaged the lung vasculature in vivo.

Behaviors of lung neutrophils

We quantified Ly6G$^+$ neutrophils using flow cytometry in whole flushed mouse lungs exsanguinated of peripheral blood and found that the percentage of neutrophils to total leukocytes was significantly higher than that in flushed liver, another highly vascular organ (Fig. 2, A and B). Using an established flow cytometry method to characterize neutrophil anatomic localization, we observed that most lung neutrophils were intravascular, with a minimum number of extravascular neutrophils under baseline conditions (fig. S3). This agrees with other reports that show that the vast majority of neutrophils in the lung are intravascular (*43*, *44*). Using pulmonary intravital microscopy, we directly visualized neutrophils within the lung vasculature and found a distribution of three behavioral phenotypes: tethering, crawling, and firm adhesion. Under basal conditions, most interactions occurred within the capillaries (vessel diameter, ≤10 μm), and no interactions were observed in vessels larger than 20 μm (Fig. 2, C and D). Some neutrophils demonstrated tethering, but none of these capture events translated into rolling. We did not observe rolling cells in these capillaries.

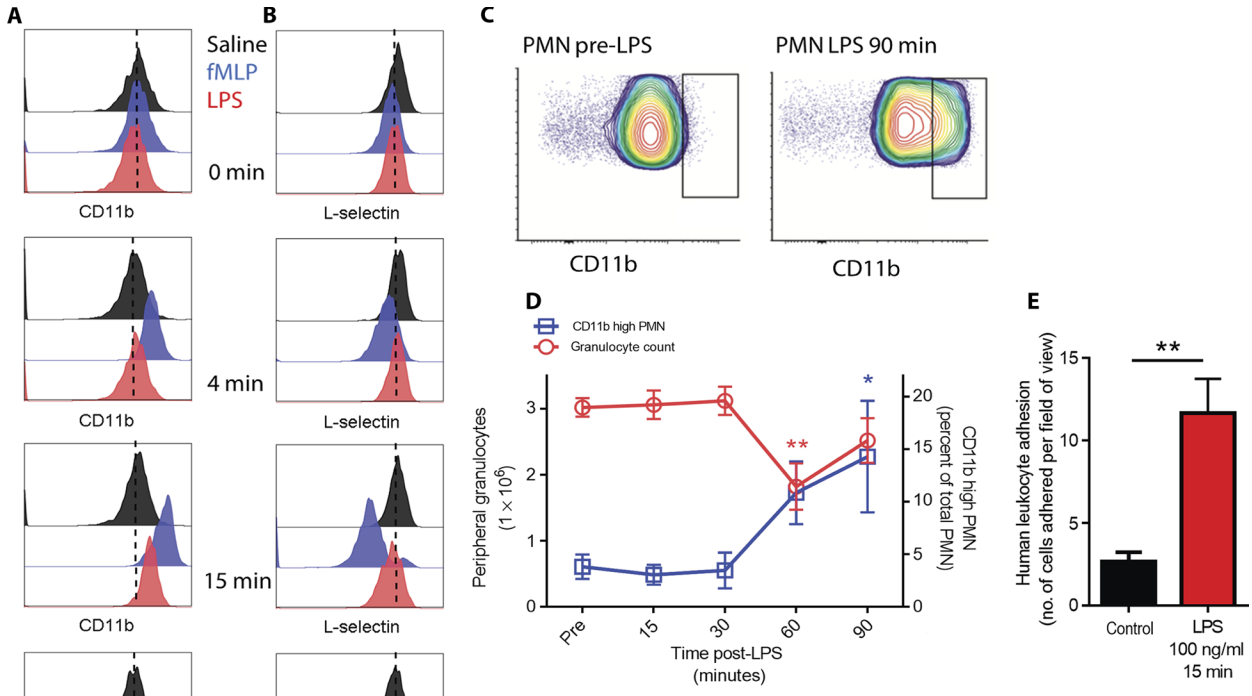

Fig. 1. LPS induces rapid cell surface increases in CD11b in mouse neutrophils and in neutrophils from humans treated with intravenous LPS. Peripheral blood leukocytes from wild-type mice were treated with either saline, fMLP (1 μM), or LPS (5 μg/ml) for 4, 15, and 30 min, and flow cytometry was performed to assess levels of cell surface expression of CD11b (**A**) and L-selectin (**B**) on $Ly6G^+$ cells (n = 3). Five healthy human volunteers received intravenous LPS, and peripheral blood was obtained over time. (**C**) Flow cytometry was performed to assess the level of cell surface CD11b before and after LPS, and the gate demonstrates $CD11b^{high}$-expressing neutrophils. PMN, polymorphonuclear leukocyte. (**D**) The total number of peripheral neutrophils from five individuals treated with LPS (left axis: means ± SEM, $^{**}P = 0.022$, n = 5, one-way ANOVA with Dunnett's correction) is graphed along with the percentage of CD11b-high cells from these individuals (right axis: means ± SEM, $^{*}P = 0.02$, n = 5, one-way ANOVA with Dunnett's correction). (**E**) Human peripheral blood leukocytes were treated with LPS (100 ng/ml; 15 min), and adhesion was assessed using a flow chamber lined with primary human pulmonary endothelium (means ± SD, $^{**}P = 0.002$, n = 3, unpaired two-tailed t test).

One-third of neutrophils crawled short distances along the vessel walls, an uncommon behavior in other untreated vascular beds (*49*–*51*). Lung capillary neutrophils were manually tracked over a 10-min duration; however, all imaging experiments were performed for at least 1 hour per mouse to allow evaluation of various fields of view (movie S1). Examples of tracks are displayed for individual neutrophils as blue lines superimposed on an intravital image or from one field of view plotted with a common origin point (Fig. 2, E and F). At baseline, capillary neutrophils crawled distances less than 20 μm (three to four cell lengths), and 35% of neutrophils did not crawl but remained stationary (adherent).

LPS rapidly induced neutrophil crawling within the pulmonary circulation

Crawling, which occurred at baseline in a third of neutrophils, rapidly and significantly increased in terms of the number of cells crawling and the distance they crawled after intravenous stimulation with LPS. Baseline crawling distance averaged 20 μm (10 min of tracking), but within 10 min of a low dose of LPS [10 μg, intravenously (iv)], neutrophil crawling distance significantly increased to an average of 38 μm (10 min of tracking) and further to 50 μm (10 min of tracking) 20 min after LPS stimulation (Fig. 3A). Tracking data were obtained in 10-min intervals; however, each individual imaging experiment lasted at least 1 hour per mouse. Neutrophils accumulated within the field of view and were significantly increased 30 min after LPS (Fig. 3B). Vascular neutrophils rapidly polarized with a lead pseudopod and a uropod tail, a phenotype that is essential before cellular mobility. Manual tracking between 20 and 30 min after LPS revealed very long crawling tracks, and vascular neutrophils were not observed to emigrate out of the microvessels (Fig. 3, C and D, and movie S2).

Basal and enhanced rapid vascular crawling behavior requires CD11b

The adhesion molecules mediating either baseline crawling or rapid LPS-stimulated crawling in the lung are unknown; however, β_2-integrins mediate crawling in inflamed muscle vasculature (*50*). The number of neutrophils demonstrating crawling under unstimulated conditions was significantly lower in *CD11b*-deficient animals (Fig. 4A) and profoundly attenuated at 30 min of LPS stimulation (Fig. 4B and movie S3), whereas the phenotype for *CD11a* deficiency was less obvious (fig. S4). Crawling distance of LPS-treated *CD11b*-deficient mice remained lower (Fig. 4, C, D, and F, and movie S3) than that of LPS-treated wild-type mice (Fig. 4, E and G). Therefore, in relation to rapid up-regulation of CD11b in mouse and human neutrophils (Fig. 1), we now have a specific biological reason for this, namely, crawling within the lung microcirculation after pathogen-related stimulation.

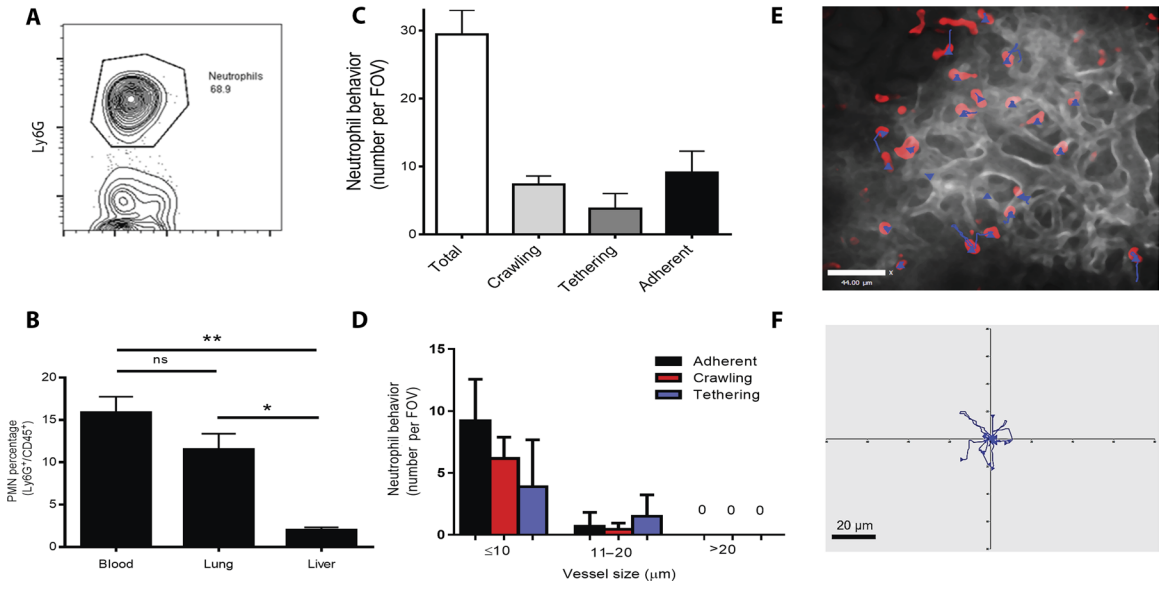

Fig. 2. Defining neutrophil behavior within the pulmonary circulation in vivo using intravital microscopy. (**A**) Ly6G$^+$ cells were quantified using flow cytometry of exsanguinated untreated C57BL/6J whole lungs. (**B**) Ly6G$^+$ cells were compared in blood, lung, and liver of untreated C57BL/6J mice (means ± SD, $^{**}P = 0.0017$, $^{*}P = 0.011$, $n = 3$, one-way ANOVA). ns, not significant. (**C**) Three neutrophil phenotypes (crawling, tethering, and adhesion) were identified in vivo using pulmonary intravital microscopy ($n = 3$). FOV, field of view. (**D**) Quantification of lung neutrophil behaviors during untreated conditions in vivo in relation to vessel diameter ($n = 3$). (**E**) Manually tracked pulmonary neutrophils in an unstimulated mouse. Neutrophils (red; intravenous fluorescently conjugated anti-Ly6G, clone 1A8), vasculature (grayscale; intravenous fluorescently conjugated anti-CD31, clone 390), and blue tracks displaying 10 min of tracking time. (**F**) Individual tracks displayed from a representative mouse over 10 min, compared from a central origin point.

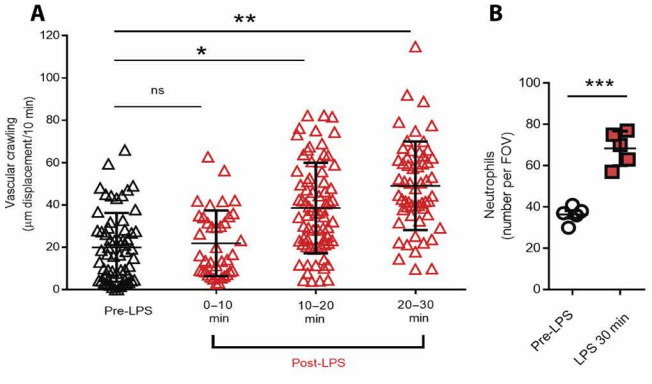

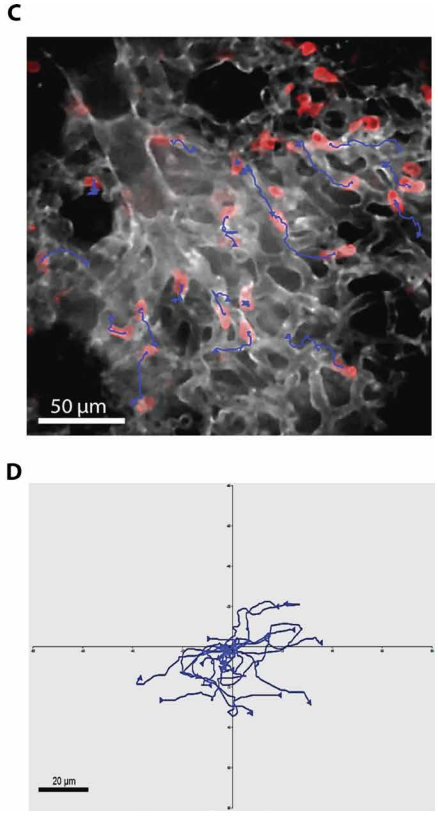

Fig. 3. Lung neutrophils rapidly begin crawling throughout the vasculature after LPS exposure. Lung neutrophils were tracked for 10 min before stimulation to quantify baseline neutrophil characteristics. (**A**) LPS (10 μg, iv) was administered, and neutrophils were tracked over time. Each symbol represents an individual neutrophil combined from three separate experiments. Statistical testing was performed by averaging crawling distance of all neutrophils tracked from each mouse and using this as a single n value (means ± SD, $^{*}P = 0.0169$, $^{**}P = 0.0014$, $n = 3$, one-way ANOVA). (**B**) Total neutrophil accumulation was quantified per field of view before and 30 min after LPS intravenous administration (means ± SD, $^{***}P = 0.0001$, $n = 5$, unpaired two-tailed t test). (**C**) A representative pulmonary intravital image with neutrophils tracked between 20 and 30 min after LPS. Neutrophils (red; fluorescently conjugated anti-Ly6G, clone 1A8; 3.5 μg per mouse, iv), vasculature (grayscale; fluorescently conjugated anti-CD31, clone 390; 5 μg per mouse, iv), and blue tracks displaying 10 min of tracking time. (**D**) Individual tracks displayed from the experiment depicted in (C). Tracks are plotted from a central common origin point.

LPS-induced rapid crawling requires TLR4 and Myd88 in vivo

Reports indicate that LPS may have non-TLR4 intracellular receptors (*52*, *53*), and perhaps these receptors mediate the nontranscriptional phenotypic changes in cellular behavior in vivo. Therefore, we initially tested whether the rapid LPS-mediated crawling is downstream of TLR4. Using pulmonary intravital microscopy, we directly visualized neutrophils in the capillaries of *Tlr4*-deficient mice during LPS intravenous challenge. There was no increase in neutrophil crawling behavior after LPS (Fig. 5, A and B), confirming that TLR4 is the major physiological pattern recognition receptor involved in this process. Myd88 is the major downstream signaling molecule for all TLRs except TLR3 and is essential for linking membrane signaling to activation of nuclear receptors and modulation of nuclear transcription. To test whether LPS-induced rapid crawling (which occurs temporally faster than gene transcription, translation, and expression) occurs via this pathway, we examined neutrophils in the lungs of *Myd88*-deficient mice using pulmonary intravital microscopy and observed no increase in LPS-induced crawling (Fig. 5, C and D). *Myd88*-deficient mice had higher basal crawling than either wild-type or *Tlr4*-deficient mice;

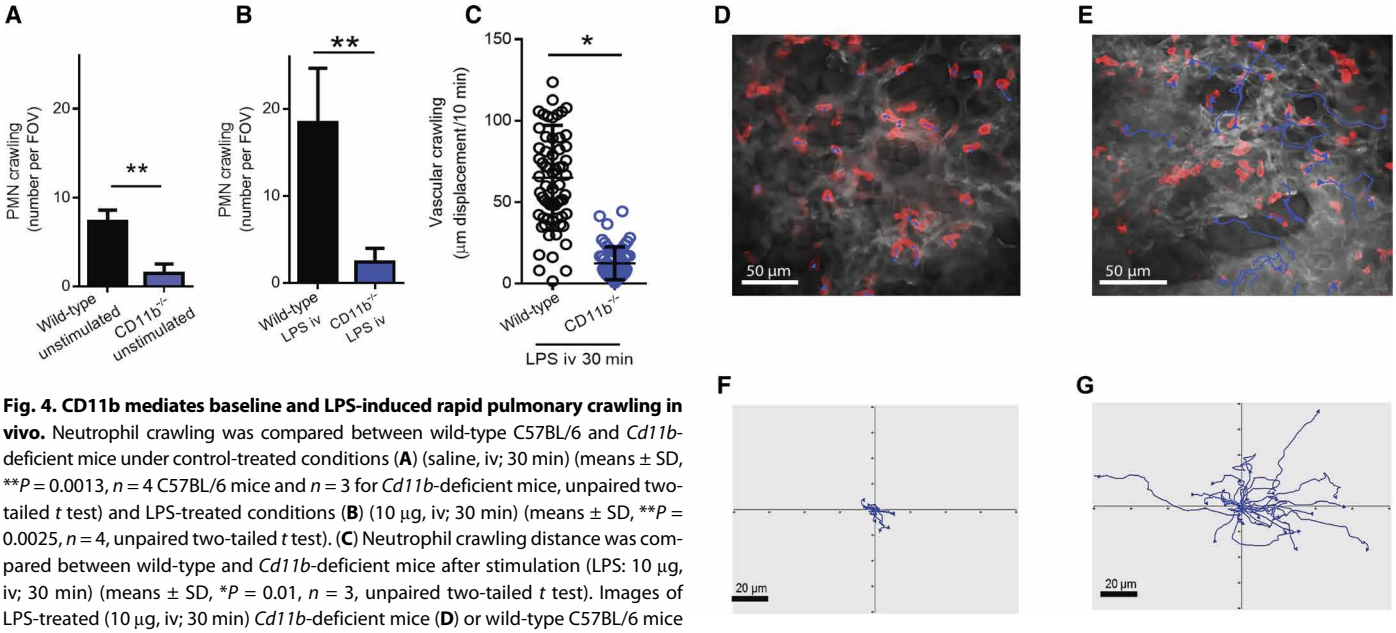

Fig. 4. CD11b mediates baseline and LPS-induced rapid pulmonary crawling in vivo. Neutrophil crawling was compared between wild-type C57BL/6 and *Cd11b*-deficient mice under control-treated conditions (**A**) (saline, iv; 30 min) (means ± SD, $^{**}P = 0.0013$, $n = 4$ C57BL/6 mice and $n = 3$ for *Cd11b*-deficient mice, unpaired two-tailed *t* test) and LPS-treated conditions (**B**) (10 μg, iv; 30 min) (means ± SD, $^{**}P = 0.0025$, $n = 4$, unpaired two-tailed *t* test). (**C**) Neutrophil crawling distance was compared between wild-type and *Cd11b*-deficient mice after stimulation (LPS: 10 μg, iv; 30 min) (means ± SD, $^{*}P = 0.01$, $n = 3$, unpaired two-tailed *t* test). Images of LPS-treated (10 μg, iv; 30 min) *Cd11b*-deficient mice (**D**) or wild-type C57BL/6 mice (**E**) from representative intravital experiments. Neutrophil tracks from LPS-treated (10 μg, iv; 30 min) wild-type mice are depicted for *Cd11b*-deficient mice (**F**) or wild-type C57BL/6 mice (**G**) from representative intravital experiments.

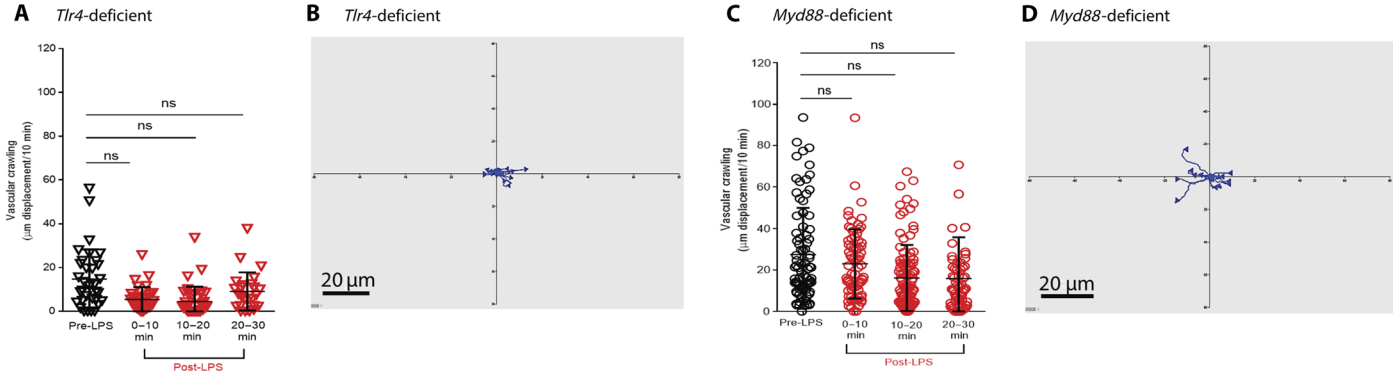

Fig. 5. Rapid neutrophil crawling is TLR4- and Myd88-dependent. Pulmonary intravital microscopy was used to directly assess the molecular requirement of rapid neutrophil crawling after LPS stimulation. *Tlr4*-deficient mice were imaged and (**A**) neutrophil crawling was quantified before and after LPS (10 μg, iv) (means ± SD, $n = 3$, one-way ANOVA, not significant). (**B**) Neutrophil tracking is displayed from a representative experiment between 20 and 30 min after LPS. *Myd88*-deficient mice were imaged, and (**C**) neutrophil crawling was quantified before and after LPS (10 μg, iv) (means ± SD, $n = 3$, one-way ANOVA, not significant). (**D**) Neutrophil tracking is displayed from a representative experiment between 20 and 30 min after LPS.

however, this was not due to differences in baseline levels of lung neutrophil CD11b expression (fig. S5).

Rapid LPS-induced neutrophil phenotype changes require abl kinase

To better understand the pathway linking Myd88 and the rapid changes in CD11b and crawling, we performed a large screen of defined pharmacological inhibitors to determine candidate targets that could inhibit LPS-mediated rapid adhesion in isolated human neutrophils (Fig. 6A). We first confirmed that rapid LPS-mediated adhesion did not require new transcription or translation (fig. S6). We next screened a pharmacological inhibitor library. The adhesion data are ordered from the lowest to the highest effect on adhesion, and the 20 least effective (black) and the 20 most effective (red) compounds are demonstrated in triplicate. Five compounds eliminated rapid LPS-activated neutrophil binding, including two different phosphatidylinositol 3-kinase (PI3K) inhibitors. Additionally, several inhibitors of p38 MAPK (mitogen-activated protein kinase) had moderate inhibitory effects. These pathways mediate neutrophil chemotaxis, making these likely targets (*54*–*56*). Two compounds, GZD824 and ponatinib, are direct and potent inhibitors of the nonreceptor tyrosine kinase abl. Abl is one of the few tyrosine kinases capable of directly binding and modulating both cytoskeletal elements and integrins in an inside-out activation model (*57*, *58*).

Our initial focus was on p38 MAPK and PI3K. Inhibition of these molecules, either by administration of a pharmacological inhibitor for p38 MAPK (Fig. 6B) or by using the *PI3K*-deficient mouse, did not inhibit LPS-dependent rapid neutrophil crawling in vivo (Fig. 6,

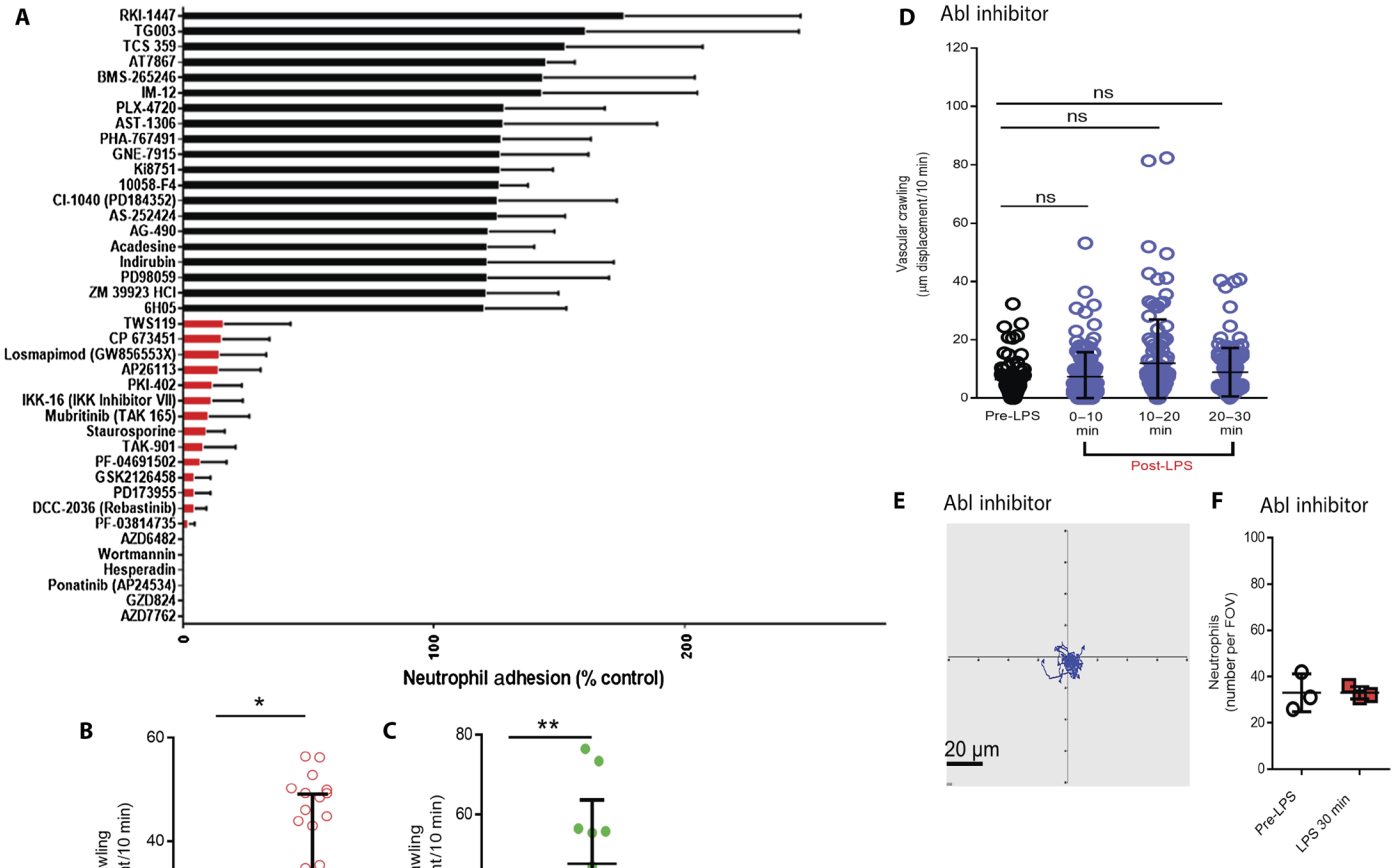

Fig. 6. The abl tyrosine kinase mediates rapid vascular crawling in vivo after LPS stimulation. (**A**) A pharmacological inhibitor screen (1 μM) was performed to assess molecules involved in rapid neutrophil adhesion after 30 min of LPS stimulation in vitro. Adhesion levels were rank-ordered, and only the 20 least effective (black) and 20 most effective inhibitors (red or absent bars) are shown. (**B**) A specific and potent p38 MAPK inhibitor (SB 239063; 10 μg/g) was administered intravenously before LPS, and vascular crawling was quantified (means ± SD, **P* = 0.018, *n* = 3, unpaired two-tailed *t* test). (**C**) Mice deficient in *PI3K* underwent pulmonary intravital before and after intravenous LPS. Vascular crawling displacement was quantified (means ± SD, ***P* = 0.066, *n* = 3, unpaired two-tailed *t* test). (**D**) Wild-type mice received GZD824, a specific abl kinase inhibitor (5 μg/g, iv) 30 min before baseline pulmonary intravital imaging. Treated mice were imaged, and neutrophil crawling was quantified (means ± SD, *n* = 3, one-way ANOVA, not significant), and (**E**) tracking was determined. (**F**) Neutrophil accumulation was quantified in mice pretreated with the abl inhibitor before and after LPS administration (means ± SD, *n* = 3, unpaired two-tailed *t* test, not significant).

B and C). This is very interesting because we have previously reported an important role for p38 MAPK and PI3K in fMLP- and chemokine-dependent crawling, respectively, in vitro and in vivo, suggesting that the LPS pathway is distinct from these chemotactic pathways (*54*, *55*, *59*, *60*). We next tested whether inhibiting abl disrupted rapid LPS-induced crawling in vivo. Mice received intravenous GZD824 (5 μg/g, iv), currently the most potent and specific pharmacological inhibitor of abl (*61*, *62*), 30 min before LPS administration. Neutrophils were incapable of enhanced crawling even after 30 min of LPS exposure (Fig. 6, D and E). Additionally, neutrophil accumulation was attenuated 30 min after LPS, unlike in LPS-treated mice that did not receive the abl inhibitor (Fig. 6F). In vitro, mouse blood neutrophils did not increase cell surface CD11b after LPS exposure when abl was inhibited (fig. S7). Abl mediates the rapid LPS-dependent up-regulation of CD11b.

Abl kinase links LPS cellular activation to CD11b expression on neutrophils in vivo

To determine whether abl directly influenced CD11b rapid expression after LPS in vivo, we used pulmonary intravital microscopy to visualize CD11b expression in $Ly6G^+$ neutrophils in mice pretreated with the abl inhibitor. After 20 min of intravenous LPS in control mice, $Ly6G^+$ cells became $CD11b^{bright}$, and overlapping $Ly6G^+/CD11b^+$ staining was visualized as yellow (Fig. 7A and movie S4). CD11b staining was predominantly observed as it accumulated in the tail and pseudopod of crawling cells, as previously reported in vitro (*63*). Animals pretreated with intravenous abl inhibitor had less visual evidence of $Ly6G^+/CD11b^+$ overlap (Fig. 7B and movie S4). Moreover, all images between 20 and 40 min after LPS were quantified for CD11b positivity using two different strategies. First, we measured the total

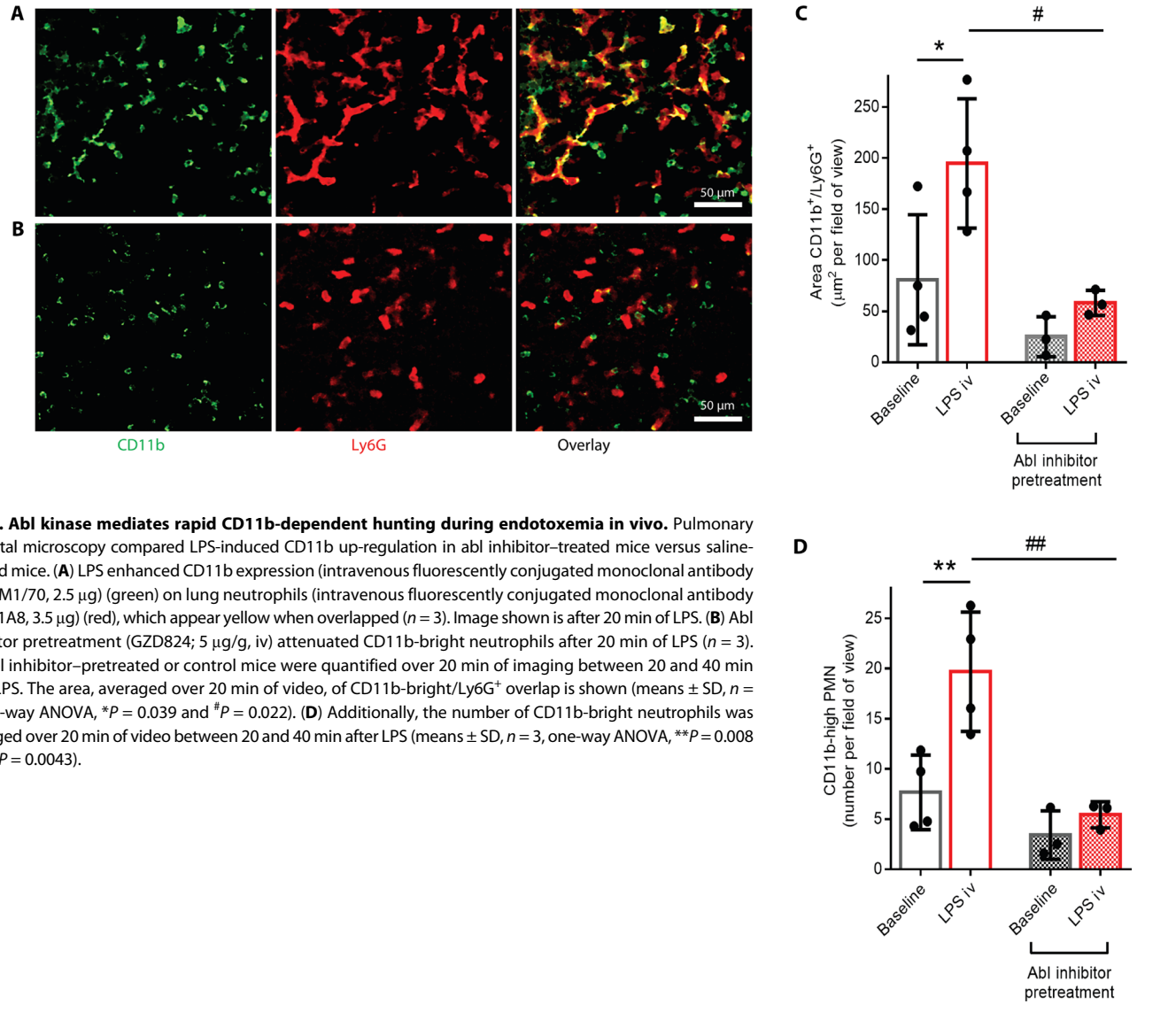

Fig. 7. Abl kinase mediates rapid CD11b-dependent hunting during endotoxemia in vivo. Pulmonary intravital microscopy compared LPS-induced CD11b up-regulation in abl inhibitor–treated mice versus saline-treated mice. (**A**) LPS enhanced CD11b expression (intravenous fluorescently conjugated monoclonal antibody clone M1/70, 2.5 μg) (green) on lung neutrophils (intravenous fluorescently conjugated monoclonal antibody clone 1A8, 3.5 μg) (red), which appear yellow when overlapped ($n = 3$). Image shown is after 20 min of LPS. (**B**) Abl inhibitor pretreatment (GZD824; 5 μg/g, iv) attenuated CD11b-bright neutrophils after 20 min of LPS ($n = 3$). (**C**) Abl inhibitor–pretreated or control mice were quantified over 20 min of imaging between 20 and 40 min after LPS. The area, averaged over 20 min of video, of CD11b-bright/Ly6G$^+$ overlap is shown (means ± SD, $n = 3$, one-way ANOVA, $^*P = 0.039$ and $^{\#}P = 0.022$). (**D**) Additionally, the number of CD11b-bright neutrophils was averaged over 20 min of video between 20 and 40 min after LPS (means ± SD, $n = 3$, one-way ANOVA, $^{**}P = 0.008$ and $^{\#\#}P = 0.0043$).

area of overlapping Ly6G$^+$ and CD11b$^+$ per field of view of each image and averaged this over 20 min of imaging (Fig. 7C). Then, we quantified the number of individual Ly6G$^+$ cells that were also CD11b$^+$ by imaging (Fig. 7D). Abl inhibition resulted in significant impairment of CD11b increases in lung neutrophils, thereby directly linking abl function to rapid neutrophil behavior in vivo through CD11b.

Rapid lung neutrophil crawling facilitates capture of bloodstream bacteria in vivo

We hypothesized that the increased vascular crawling phenotype may be a surveillance system providing immediate detection and capture of lung-sequestered bacteria that are no longer in free circulation. Therefore, we tested whether rapid pulmonary neutrophil crawling facilitated the capture of blood-borne pathogens. *E. coli* remains the most common cause of bacteremia in humans, and it is the prototypical pathogen associated with LPS-TLR4–mediated host defense. A simple model of bacteremia, using a live, fluorescently conjugated human clinical *E. coli* isolate (*64*) injected intravenously, was directly imaged in the lung circulation. Bacteria rapidly sequestered within the lung vasculature by adhering to the vessel wall (Fig. 8A and movie S5). More than 50% of the total visualized pathogens adhered to the vessel wall during the first minute (Fig. 8B). Macrophages are classically involved in sequestering circulating particles and pathogens (*28*). However, mice and humans do not have resident intravascular pulmonary macrophage (*65*, *66*). We could not detect any intravascular macrophage using pulmonary intravital and fluorescently labeled antibodies either against macrophage or in the *lysm-EGFP* transgenic mice; nevertheless, we depleted all macrophages using systemic clodronate liposomes, and *E. coli* continued to adhere to the vessel walls (Fig. 8C). Deletion of CRIg, a receptor on intravascular macrophage and the molecule critical for bacterial capture by macrophage in liver (*26*, *28*), again failed to prevent bacterial binding to pulmonary endothelium (Fig. 8D). Additionally, after neutrophil depletion, bacteria remained unperturbed by any other immune cells within the vasculature for as long as we could image (Fig. 8E). As such, the data suggest that bacteria adhered to the endothelium and not to macrophage or neutrophils and that neutrophils were chiefly responsible for immediate capture.

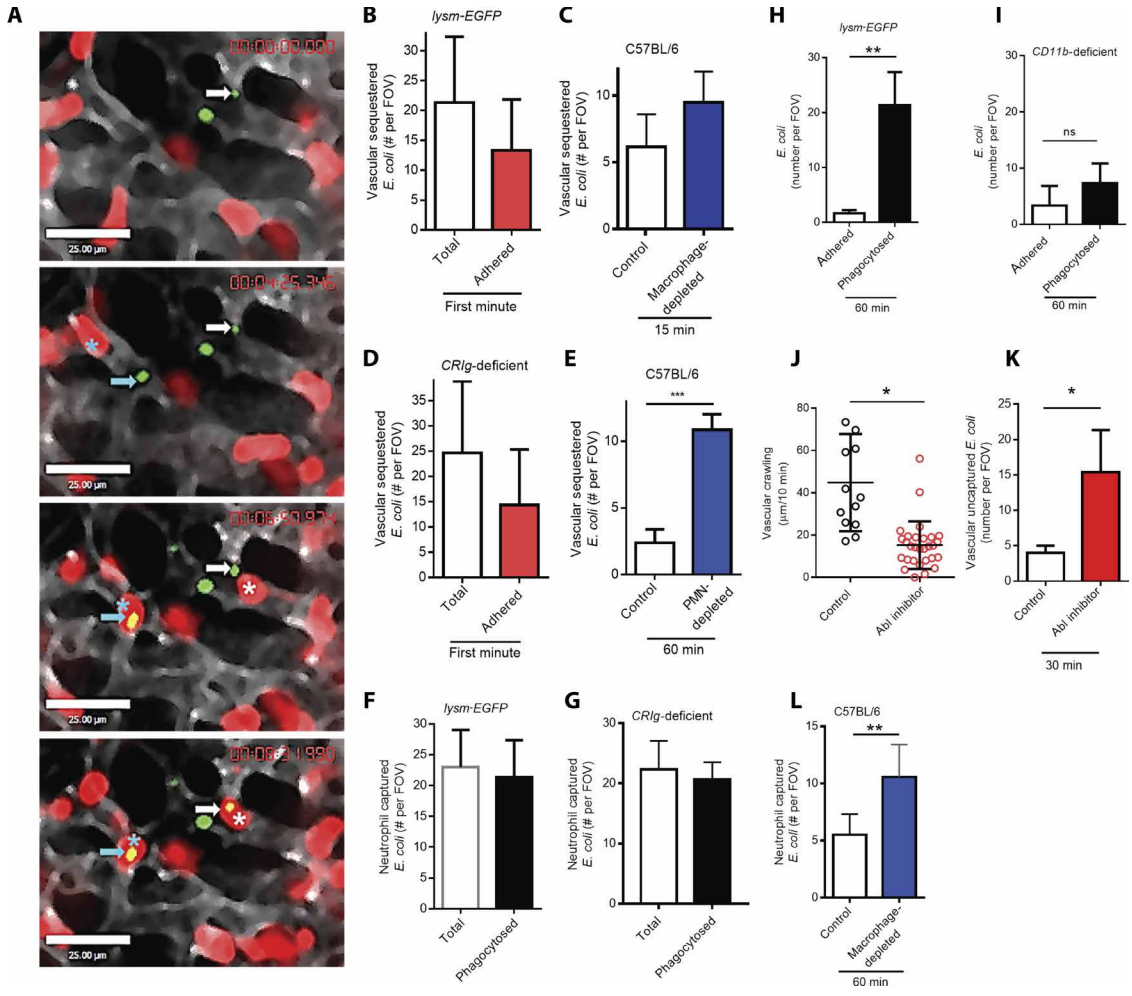

Fig. 8. The lung provides a niche for rapid neutrophil surveillance and capture of bloodstream bacteria in vivo. (**A**) Crawling neutrophil behavior was directly examined using a model of *E. coli* Gram-negative bacteremia. Fluorescently labeled transgenic *E. coli* was administered (1×10^7 colony-forming units, iv) at the time of imaging using the *lysm-EGFP* mouse. The sequence of images demonstrates endothelial capture of *E. coli* and, subsequently, two separate neutrophil capture events. Arrows highlight bacteria, whereas the corresponding neutrophil is marked with color-coded asterisks. (**B**) Bacteria trapped along the vasculature of *lysm-EGFP* during the first pass are compared with the total number of bacteria visualized during the first pass (means ± SD, $n = 3$, unpaired two-tailed t test, not significant). (**C**) *E. coli* vascular sequestration was observed in macrophage-depleted C57BL/6J or control mice (means ± SD, $n = 5$, unpaired two-tailed t test, not significant). (**D**) Bacteria trapped along the vasculature of *CRIg*-deficient mice during the first pass are compared with the total number of bacteria visualized during the first pass (means ± SD, $n = 5$, unpaired two-tailed t test, not significant). (**E**) *E. coli* sequestration in neutrophil-depleted C57BL/6J versus control C57BL/6J (means ± SD, $n = 5$, unpaired two-tailed t test, $^{***}P = 0.001$). *E. coli* captured by lung neutrophils compared with the total bacteria per field of view was quantified after 60 min of bacteria administration in either *lysm-EGFP* mice (**F**) (means ± SD, $n = 3$, unpaired two-tailed t test, not significant) or *CRIg*-deficient mice (**G**) (means ± SD, $n = 3$, unpaired two-tailed t test, not significant). After 60 min of bacteria administration, the number of *E. coli* remaining adhered to the vessel wall versus phagocytosed by neutrophils is demonstrated in *lysm-EGFP* mice (**H**) (means ± SD, $n = 3$, unpaired two-tailed t test, $^{**}P = 0.0049$) and *CD11b*-deficient mice (**I**) (means ± SD, $n = 3$, unpaired two-tailed t test, not significant). (**J**) Neutrophil crawling was quantified as the vascular distance between 20 and 30 min after intravenous *E. coli* in control C57BL/6J mice versus mice pretreated with the abl inhibitor (GZD824; 5 μg/g, iv) (mean ± SD, $n = 3$, unpaired two-tailed t test, $^{*}P = 0.032$). (**K**) The number of freely circulating uncaptured bacteria was quantified in control and abl inhibitor–treated mice after 30 min of bacteremia (means ± SD, $n = 3$, unpaired two-tailed t test, $^{*}P = 0.018$). (**L**) Bacteria capture by neutrophils was determined after 60 min of *E. coli* administration in control mice versus macrophage-depleted mice (means ± SD, $n = 3$, unpaired two-tailed t test, $^{**}P = 0.009$).

Similar to LPS treatment, neutrophils in the capillary vessels rapidly polarized and began to crawl throughout the vasculature, ultimately targeting the sequestered *E. coli*. Figure 8A demonstrates two examples of neutrophil rapidly initiating crawling, which leads to bacterial capture. Crawling that resulted in capture is demonstrated on the left side of the screen and marked by a blue asterisk and arrow, whereas the right side demonstrates the second neutrophil crawling and capturing event, highlighted by a white asterisk and arrow (Fig. 8A and movie S5). The number of *E. coli* adhered to vessels decreased over time, because the majority of visualized bacteria were phagocytosed by vascular neutrophils (Fig. 8F). Neutrophils in CRIg-deficient mice also efficiently phagocytosed sequestered bacteria (Fig. 8G). Furthermore, few bacteria remained free of neutrophil capture along the vessel wall at 1 hour in *lysm-EGFP* mice because most were now phagocytosed (Fig. 8H). However, in *CD11b*-deficient mice, where neutrophils could not crawl to efficiently reach the *E. coli*, low numbers of bacteria were phagocytosed (Fig. 8I). We studied the process of neutrophil-mediated rapid crawling and *E. coli* capture in both transgenically labeled myeloid cells (*lysm-EGFP*; Fig. 8, A, B, F, and H, and movie S5) and fluorescently labeled specific antibodies toward neutrophils (clone 1A8), and no differences were observed. The abl inhibitor impaired *E. coli*–induced rapid crawling in vivo (Fig. 8J), similar to our previous LPS experiments. The abl inhibitor also impaired the ability of the capillary neutrophils to capture vascular bacteria, leading to an increase in uncaptured but vascular-adhered *E. coli* (Fig. 8K). In a final experiment, depletion of macrophage did not impair the

neutrophil phagocytosis in the lung (Fig. 8L). Together, we have demonstrated a host defense system whereby neutrophils are rapidly activated upon pathogen detection to survey the pulmonary vasculature for bloodstream infections sequestered in the pulmonary microvasculature. Hence, the lung capillaries provide a host defense niche for immediate neutrophil patrolling and capture of bloodstream bacteria.

DISCUSSION

Systemic infections, whereby the pathogen enters the bloodstream, have worse outcomes than focal and localized infections. Even for sepsis, which has an incredibly high mortality, the outcomes are worse if bacteremia occurs (*2*). Conventional paradigms consider that most bloodstream invaders are cleared via specialized stationary mononuclear phagocytes in the liver and spleen. Yet, the major risk factor for developing a bloodstream infection is the lack of, or dysfunction of, neutrophils (*29*, *30*). Here, we report two findings concerning neutrophil-mediated host defense and establish the lung as an important organ involved in vascular defense with unique contributions that differ from conventional macrophage-dominant defense in the liver and spleen.

Endotoxin triggers immediate changes in host physiology; however, functionally relevant nontranscriptional cellular behaviors after LPS-TLR4 activation either in vivo or in vitro are underreported. In humans and mice treated with LPS, changes in vital signs, such as fever or tachycardia, occur after 2 hours (*67*–*70*). Additionally, the appearance of proinflammatory cytokines interleukin-6 or TNF-α or changes in leukocyte counts also require hours. In contrast to the reported downstream mechanisms of LPS-TLR4 that require hours, we found a physiologically relevant in vivo host defense mechanism that occurs within minutes of LPS and requires TLR4. In vivo, neutrophils were immediately triggered to search the vast capillary network in a CD11b-dependent manner. After TLR4 and Myd88 signal transduction, CD11b-mediated crawling required abl kinase. The role of this kinase was revealed using a pharmacological inhibition library to assess unbiased pathways in rapid LPS-mediated adhesion. Although other kinases are also involved in neutrophil adhesion and migration, including Src and Syk (*71*–*74*), the functional relevance of kinase activation directly linked to rapid behavioral activation in vivo is less appreciated. We observed that abl mediates an inside-out neutrophil activation pathway, leading to CD11b-dependent crawling, that is important in immediate vascular host defense. Further confirmation of this rapid TLR4-dependent neutrophil activation was the shedding of L-selectin within minutes after LPS exposure. There has been some suggestion that LPS can rapidly activate immune cells. Neutrophils adhere rapidly to artificial substrata when given LPS (*22*, *45*). Recently, the macrophage secretosome was mapped downstream of LPS stimulation. Using proteomics, they found that numerous proteins were nontranscriptionally secreted after LPS; however, this only peaked after 8 hours (*75*). Nevertheless, these studies support our view that TLR4 can mediate cellular responses, both transcriptionally and nontranscriptionally. We previously found that bacteria could trigger NETosis via TLR4 on platelets (*64*, *76*), yet by using pulmonary intravital microscopy, we could not observe any NET structures in the capillaries after bacterial stimulation.

Neutrophils can marginate and recruit to the lung under basal conditions (*77*, *78*), yet the functional relevance of this large cohort of innate cells has remained obscure. Our data demonstrate that the large populations of transient and marginated neutrophils are poised to immediately eliminate sequestered pathogens. Therefore, we have found an in vivo host defense system that deals with bloodstream infections independent of the mononuclear phagocyte system and supports the clinical finding that neutropenia predisposes to disseminated bloodstream infection.

CD11b is critical to neutrophil-mediated host defense. A major role of this integrin is to mediate neutrophil adhesion and migration. Selective β_2-integrin–mediated recruitment is regulated by multiple mechanisms, including increased cell surface expression and changes in the extracellular activation state (*79*). Examples that demonstrate the importance of deficiencies in cell surface CD11b as well as impairments in activation of CD11b exist. Patients with severely depressed β_2-integrin cell surface levels develop severe invasive bloodstream infections and sepsis (*80*). In humans or mice with Wiskott-Aldrich syndrome, a primary immunodeficiency characterized by recurrent bacterial infections, neutrophils have both impairment in integrin-induced activation and an impaired ability of CD11b to properly polarize to the uropod, thereby impairing adhesion and cell migration (*81*). Similarly, leukocyte adhesion deficiency type III (a human condition in which the molecule kindlin-3, which binds the common integrin β chain and mediates CD11b activation and adhesion in vitro, is missing) is also characterized by bacterial infections (*82*–*84*). Our in vivo imaging identified that increases in cell surface CD11b are required for rapid crawling and patrolling behaviors in the lung, a common place for infections. Although both our human and mouse in vivo and our in vitro models demonstrate overall increases in CD11b, we cannot rule out the possibility that the activation state may also be rapidly changed after LPS.

Abl kinase has not specifically been shown to mediate rapid CD11b-mediated neutrophil host defense, yet there is precedence linking this kinase to integrin function and neutrophil adhesion. The abl nonreceptor tyrosine kinase is notable for its role in chronic myelogenous leukemia (CML) as BCR-abl. Under nonmalignant conditions, abl is only one of two kinases that are known to directly bind and interact with the cytoskeleton and mediate cell migration and polarity (*57*). Growth factors stimulate abl through Src kinase activation, and β_2-integrin adhesion can stimulate abl via Src and Syk. The Wiskott-Aldrich syndrome proteins, implicated in CD11b impairment, are activated via abl kinase (*57*). Moreover, abl kinases can activate Vav1, a molecule known to mediate neutrophil migration (*49*), at the pseudopod leading edge during β_2-integrin crawling in neutrophils, and inhibiting abl impairs recruitment in a peritonitis model (*72*, *73*). Dasatinib, a clinical drug used to treat CML, inhibits several tyrosine kinases, including abl and Src. This drug inhibits neutrophil chemotaxis and adhesion-mediated functions, although the relationship to integrin function is unclear (*71*). In our model, abl kinase was necessary to increase CD11b expression presumably through granule mobilization and secretion, where CD11b is stored.

Several limitations of this study require further investigation. The mechanistic differences observed in the pulmonary vasculature compared with other vascular beds, in terms of sequestering bacteria and supporting rapid neutrophil crawling, remain obscure. Specifically, we could not identify how bacteria adhere to the endothelium and whether this is related to adhesion molecules or vascular architecture. Additionally, the endothelial molecules responsible for mediating rapid neutrophil recruitment in the lung, but not in other microvascular beds such as dermal endothelium, have not been resolved. Endothelium is heterogenous and diverse throughout the different organs of the body. Another limitation is that it remains unclear what the exact relationship is between Myd88, abl kinase, and the process of CD11b up-regulation. Direct measurement of abl kinase activity in primary lung neutrophils from mice is challenging, and so far, the only example of measuring abl

kinase activity in granulocytes has required HL-60 cell lines in vitro (*72*). Last, deficiency of CD11b, a subunit of the β_2-integrin adhesion molecule family, could lead to compensatory changes in the other chains, such as CD11a, CD11c, and CD11d. However, we have not methodically tested whether compensatory expression of other β_2-integrin chains could be affected in *CD11b*-deficient mice.

Overall, this study opens new areas of host defense and inflammation research and highlights a neutrophil surveillance and capture behavior in vivo. Additionally, it establishes that the lung microvascular system is not solely involved in gas exchange but is an important host defense niche for neutrophils distinct from the conventional monophagocytic systems of the liver and spleen.

MATERIALS AND METHODS

Study design

This study used an in vivo mouse model of intravital imaging to assess neutrophil host defense. A sample size calculation was not performed a priori because the effect sizes of our observations and interventions could not be determined before experimentation. This study was not randomized and was not blinded.

Reagents

Highly purified LPS from *E. coli* O111:B4 was purchased from List Biological Industries Inc. Fluorescently conjugated anti-Ly6G antibodies (clone 1A8, Alexa 594 and Alexa 647) and anti-CD31 antibodies (clone 390, Alexa 594 and Alexa 647) were purchased from BioLegend, eBioscience, and BD Biosciences. *E. coli*, isolated from a patient with meningitis, was previously transfected with an mTomato-fluorescent reporter (*64*). The Abl-specific inhibitor GZD824 Dimesylate was purchased from Selleck Chemicals. Previous in vivo studies found abl inhibition with 5 to 10 μg/g per day for 6 days or 25 μg/g per day for 2 weeks (*61*, *62*).

Inhibitor screen

Human neutrophils (5×10^6/ml) were labeled with calcein-AM (1 μM final concentration; Molecular Probes) for 30 min at 37°C, washed twice, and resuspended in Hepes buffer at a concentration of 2×10^6/ml. Adhesion was determined in an uncoated 96-well MaxiSorp plate (Nunc), which has a high affinity for proteins. After preincubation with dimethyl sulfoxide or the different compounds at the indicated concentrations for 15 min at 37°C, calcein-labeled cells (2×10^5 per well; final volume, 100 μl) were stimulated with bacterial TLR4 ligand LPS (20 ng/ml) (isolated from the *E. coli* strain 055:B5; Sigma-Aldrich) in the presence of LPS-binding protein (50 ng/ml) (R&D Systems). Plates were incubated for 30 min at 37°C and washed three times with phosphate-buffered saline (PBS). Adherent cells were lysed in 0.5% (w/v) Triton X-100 in H_2O for 5 min at room temperature. Fluorescence was measured with a GENios plate reader at an excitation wavelength of 485 nm and an emission wavelength of 535 nm (*82*).

LPS administration to human volunteers

Patients were enrolled after screening and prehydrated as previously reported (*85*). U.S. reference *E. coli* endotoxin (lot Ec-5; Center for Biologics Evaluation and Research, Food and Drug Administration, Bethesda, MD, USA) was used in this study. Endotoxin was reconstituted in 5 ml of saline and injected as a single intravenous bolus for 1 min at $t = 0$. Blood samples anticoagulated with sodium heparin were taken from the arterial catheter. The study protocol concerning the human endotoxemia challenges was approved by the Ethics Committee of the Radboud University Nijmegen Medical Centre and complies with the Declaration of Helsinki and the Good Clinical Practice guidelines. Volunteers gave written informed consent. The Ethics Committee of the University Medical Center Utrecht approved the study protocol. Patients gave informed consent after sampling of the blood according to the research protocol. For human flow cytometry, white blood cell differential counts were performed on a CELL-DYN Emerald hemocytometer. After blood withdrawal, red blood cells were lysed immediately (150 mM NH_4Cl, 10 mM $KHCO_3$, and 0.1 mM Na_2EDTA), followed by antibody staining in PBS2+ (0.32% trisodium citrate and 10% human pasteurized plasma solution), followed by fixation (1% formaldehyde). Fluorescence-activated cell sorting was performed on a BD Fortessa with fluorescently conjugated antibodies against CD35, CD16 (Becton Dickinson), and CD11b (Dako).

Animals

Mice were housed at the University of Calgary in a specific pathogen–free facility and used under a specific institutional review board–approved ethics protocol. C57BL/6J mice were purchased from the Jackson Laboratory (Maine, USA). *CD11b*-, *Tlr4*-, and *Myd88*-deficient and *lysm-EGFP* colonies were maintained at the University of Calgary. Mice (20 to 35 g, 6 to 10 weeks old) were housed in a pathogen-free environment and had access to food and water ad libitum. All procedures performed were approved by the University of Calgary Animal Care Committee and were in accordance with the Canadian Guidelines for Animal Research.

Pulmonary intravital microscopy

Stabilized pulmonary intravital microscopy has been previously reported (*86*). This technique was learned at University of California, San Francisco in the Krummel laboratory and performed with minor alterations related to fluorescently conjugated antibodies and the microscopes used at the University of Calgary. Briefly, anesthetized mice (ketamine and xylazine) received a right internal jugular intravenous catheter to administer fluorescent antibodies, anesthetics, and inhibitors. Some experiments used *lysm-EGFP* mice to visualize neutrophils and monocytes. To visualize the endothelium, 5 μg of fluorescently conjugated anti-CD31 antibody (clone 390, BioLegend; either Alexa 594 or Alexa 647) was administered intravenously 10 min before imaging. For experiments using nonfluorescent mice (C57BL/6J *CD11b*-, *Tlr4*-, and *Myd88*-deficient), 3.5 μg of fluorescently conjugated anti-Ly6G antibody (clone 1A8, BioLegend; either Alexa 594 or Alexa 647) was injected intravenously, to specifically visualize neutrophils at the same time as fluorescently conjugated anti-CD31 antibody. A tracheostomy is performed, and the mouse is ventilated at a tidal volume of 10 μl/g and a rate between 120 and 130, with entrained oxygen and a positive end-expiratory pressure of 4 cm H_2O. To avoid volutrauma and barotrauma, mice in our experiments were subjected to tidal volumes between 180 and 240 μl, compared with previous reports that used 500 μl per tidal volume (*42*). The left lung is exposed after a thoracotomy and rib resection, and the vacuum chamber is applied to facilitate imaging. Intravital microscopy was performed with either a spinning-disk microscope (Quorum) or a resonant scanning confocal microscope (Leica). Spinning-disk confocal intravital microscopy was performed using an Olympus BX51 upright microscope (Olympus) equipped with a 20×/0.95 XLUM Plan Fl water immersion objective. The microscope was equipped with a confocal

light path (WaveFx, Quorum) based on a modified Yokogawa CSU-10 head (Yokogawa Electric Corporation). Laser excitation at 488, 561, and 649 nm was used in rapid succession, and fluorescence in green, red, and blue channels was visualized with the appropriate long-pass filters (Semrock). A 512 × 512–pixel back-thinned EMCCD (electron-multiplying charge-coupled device) camera (C9100-13, Hamamatsu) was used for fluorescence detection. Resonant scanning (8 Hz) confocal was performed with an upright Leica SP8 equipped with a white light laser and three HyD spectral detectors and a 25× water objective with a numerical aperture of 0.9. All imaging experiments were carried out for a minimum of 1 continuous hour. Images were acquired every 10 s, and a new field of view was chosen after 20 min of observation. Therefore, at least three fields of view were observed for every 1-hour imaging experiment. Images were processed and analyzed in Volocity 4.20.

Neutrophil behavior analysis

Neutrophil behavior was analyzed offline using Volocity 4.20. Cellular enumeration and tracking were performed manually. For phenotypic quantification, tethering was defined as a discrete neutrophil interaction with the vascular wall, which arrests its circulatory movement for less than 30 s. Crawling was defined as continuous interaction of a neutrophil with the vascular wall for more than 30 s, which involves a polarized cell that does not remain stationary. Adhesion was defined as a stationary neutrophil that was not mobile and remained static for at least 30 s (*46*, *49*, *50*, *87*, *88*). Velocity, distance, and track crawling for individual neutrophils were determined manually using Volocity software. Individual neutrophils were tracked in 10-min intervals.

Statistics

Data were analyzed using GraphPad Prism software for Windows version 6.02. Data are presented as either means ± SEM or means ± SD. For figures comparing two groups of data, two-tailed unpaired *t* test was used. For figures comparing more than two groups, one-way analysis of variance (ANOVA) with Tukey's multiple comparisons tests was used. For the human intravenous LPS experiments, data were analyzed using repeated-measures ANOVA with Dunnett's correction for multiplicity. Flow cytometry data were analyzed using FlowJo v10. For all experiments, *n* represents the number of individual experiments performed.

SUPPLEMENTARY MATERIALS

immunology.sciencemag.org/cgi/content/full/2/10/eaam8929/DC1
Fig. S1. Flow cytometry gating strategy for neutrophils.
Fig. S2. Cell surface versus intracellular CD11b after LPS.
Fig. S3. Dual antibody labeling reveals neutrophil anatomic compartmentalization in the lung using flow cytometry.
Fig. S4. CD11b deficiency has a greater impact on rapid LPS-mediated crawling in the lung.
Fig. S5. CD11b expression in lung neutrophils from wild-type and *Myd88*-deficient mice.
Fig. S6. Rapid LPS-mediated neutrophil adhesion does not require transcription or translation.
Fig. S7. Rapid LPS-induced up-regulation of CD11b requires abl kinase.
Movie S1. Baseline neutrophil behaviors in unstimulated mouse lung in vivo.
Movie S2. LPS initiates a rapid neutrophil crawling behavior in vivo.
Movie S3. LPS-stimulated rapid neutrophil crawling requires CD11b in vivo.
Movie S4. Abl inhibition impairs rapid lung neutrophil CD11b expression after LPS in vivo.
Movie S5. Neutrophils in the lung rapidly respond and capture bloodstream microbial invaders.
Source data

REFERENCES AND NOTES

1. V. Liu, G. J. Escobar, J. D. Greene, J. Soule, A. Whippy, D. C. Angus, T. J. Iwashyna, Hospital deaths in patients with sepsis from 2 independent cohorts. *JAMA* **312**, 90–92 (2014).
2. A. Mansur, Y. Klee, A. F. Popov, J. Erlenwein, M. Ghadimi, T. Beissbarth, M. Bauer, J. Hinz, Primary bacteraemia is associated with a higher mortality risk compared with pulmonary and intra-abdominal infections in patients with sepsis: A prospective observational cohort study. *BMJ Open* **5**, e006616 (2015).
3. K. B. Laupland, Incidence of bloodstream infection: A review of population-based studies. *Clin. Microbiol. Infect.* **19**, 492–500 (2013).
4. E. Biondi, R. Evans, M. Mischler, M. Bendel-Stenzel, S. Horstmann, V. Lee, J. Aldag, F. Gigliotti, Epidemiology of bacteremia in febrile infants in the United States. *Pediatrics* **132**, 990–996 (2013).
5. J. Deen, L. von Seidlein, F. Andersen, N. Elle, N. J. White, Y. Lubell, Community-acquired bacterial bloodstream infections in developing countries in south and southeast Asia: A systematic review. *Lancet Infect. Dis.* **12**, 480–487 (2012).
6. M. L. Metersky, G. Waterer, W. Nsa, D. W. Bratzler, Predictors of in-hospital vs postdischarge mortality in pneumonia. *Chest* **142**, 476–481 (2012).
7. M. Magret, T. Lisboa, I. Martin-Loeches, R. Máñez, M. Nauwynck, H. Wrigge, S. Cardellino, E. Díaz, D. Koulenti, J. Rello; EU-VAP/CAP Study Group, Bacteremia is an independent risk factor for mortality in nosocomial pneumonia: A prospective and observational multicenter study. *Crit. Care* **15**, R62 (2011).
8. W. Sligl, G. Taylor, P. G. Brindley, Five years of nosocomial Gram-negative bacteremia in a general intensive care unit: Epidemiology, antimicrobial susceptibility patterns, and outcomes. *Int. J. Infect. Dis.* **10**, 320–325 (2006).
9. D. J. Diekema, S. E. Beekmann, K. C. Chapin, K. A. Morel, E. Munson, G. V. Doern, Epidemiology and outcome of nosocomial and community-onset bloodstream infection. *J. Clin. Microbiol.* **41**, 3655–3660 (2003).
10. P. Retamar, M. D. López-Prieto, C. Nátera, M. de Cueto, E. Nuño, M. Herrero, F. Fernández-Sánchez, A. Muñoz, F. Téllez, B. Becerril, A. García-Tapia, I. Carazo, R. Moya, J. E. Corzo, L. León, L. Muñoz, J. Rodríguez-Baño; Sociedad Andaluza de Enfermedades Infecciosas/Sociedad Andaluza de Microbiología y Parasitología Clínica and Red Española de Investigación en Enfermedades Infecciosas (SAEI/SAMPAC/REIPI) Bacteremia Group, F. Rodríguez-López, M. V. García, V. Fernández-Galán, A. del Arco, M. J. Pérez-Santos, A. Sánchez Porto, M. Torres-Tortosa, A. Martín-Aspas, A. Arroyo, C. García-Figueras, F. Acosta, C. Florez, P. Navas, T. Escobar-Lara, Reappraisal of the outcome of healthcare-associated and community-acquired bacteramia: A prospective cohort study. *BMC Infect. Dis.* **13**, 344 (2013).
11. J. D. D. Pitout, K. B. Laupland, Extended-spectrum β-lactamase-producing Enterobacteriaceae: An emerging public-health concern. *Lancet Infect. Dis.* **8**, 159–166 (2008).
12. P. Savard, T. M. Perl, A call for action: Managing the emergence of multidrug-resistant Enterobacteriaceae in the acute care settings. *Curr. Opin. Infect. Dis.* **25**, 371–377 (2012).
13. A. Kumar, D. Roberts, K. E. Wood, B. Light, J. E. Parrillo, S. Sharma, R. Suppes, D. Feinstein, S. Zanotti, L. Taiberg, D. Gurka, A. Kumar, M. Cheang, Duration of hypotension before initiation of effective antimicrobial therapy is the critical determinant of survival in human septic shock. *Crit. Care Med.* **34**, 1589–1596 (2006).
14. A. Poltorak, X. He, I. Smirnova, M.-Y. Liu, C. Van Huffel, X. Du, D. Birdwell, E. Alejos, M. Silva, C. Galanos, M. Freudenberg, P. Ricciardi-Castagnoli, B. Layton, B. Beutler, Defective LPS signaling in C3H/HeJ and C57BL/10ScCr mice: Mutations in *Tlr4* gene. *Science* **282**, 2085–2088 (1998).
15. R. Medzhitov, T. Horng, Transcriptional control of the inflammatory response. *Nat. Rev. Immunol.* **9**, 692–703 (2009).
16. T. Kawai, S. Akira, The role of pattern-recognition receptors in innate immunity: Update on Toll-like receptors. *Nat. Immunol.* **11**, 373–384 (2010).
17. T. Kawai, S. Akira, Toll-like receptors and their crosstalk with other innate receptors in infection and immunity. *Immunity* **34**, 637–650 (2011).
18. M. J. Hickey, P. Kubes, Intravascular immunity: The host-pathogen encounter in blood vessels. *Nat. Rev. Immunol.* **9**, 364–375 (2009).
19. E. Kolaczkowska, P. Kubes, Neutrophil recruitment and function in health and inflammation. *Nat. Rev. Immunol.* **13**, 159–175 (2013).
20. D. Ricklin, G. Hajishengallis, K. Yang, J. D. Lambris, Complement: A key system for immune surveillance and homeostasis. *Nat. Immunol.* **11**, 785–797 (2010).
21. T. K. Kishimoto, M. A. Jutila, E. L. Berg, E. C. Butcher, Neutrophil Mac-1 and MEL-14 adhesion proteins inversely regulated by chemotactic factors. *Science* **245**, 1238–1241 (1989).
22. G. S. Worthen, N. Avdi, S. Vukajlovich, P. S. Tobias, Neutrophil adherence induced by lipopolysaccharide in vitro. Role of plasma component interaction with lipopolysaccharide. *J. Clin. Invest.* **90**, 2526–2535 (1992).
23. B. N. Halpern, The role and function of the reticulo-endothelial system in immunological processes. *J. Pharm. Pharmacol.* **11**, 321–338 (1959).

24. S. J. Jenkins, D. A. Hume, Homeostasis in the mononuclear phagocyte system. *Trends Immunol.* **35**, 358–367 (2014).
25. D. A. Hume, The mononuclear phagocyte system. *Curr. Opin. Immunol.* **18**, 49–53 (2006).
26. K. Y. Helmy, K. J. Katschke Jr., N. N. Gorgani, N. M. Kljavin, J. M. Elliott, L. Diehl, S. J. Scales, N. Ghilardi, M. van Lookeren Campagne, CRIg: A macrophage complement receptor required for phagocytosis of circulating pathogens. *Cell* **124**, 915–927 (2006).
27. W.-Y. Lee, T. J. Moriarty, C. H. Y. Wong, H. Zhou, R. M. Strieter, N. van Rooijen, G. Chaconas, P. Kubes, An intravascular immune response to *Borrelia burgdorferi* involves Kupffer cells and *i*NKT cells. *Nat. Immunol.* **11**, 295–302 (2010).
28. Z. Zeng, B. G. J. Surewaard, C. H. Y. Wong, J. A. Geoghegan, C. N. Jenne, P. Kubes, CRIg functions as a macrophage pattern recognition receptor to directly bind and capture blood-borne Gram-positive bacteria. *Cell Host Microbe* **20**, 99–106 (2016).
29. G. P. Bodey, M. Buckley, Y. S. Sathe, E. J. Freireich, Quantitative relationships between circulating leukocytes and infection in patients with acute leukemia. *Ann. Intern. Med.* **64**, 328–340 (1966).
30. L. S. Elting, E. B. Rubenstein, K. V. I. Rolston, G. P. Bodey, Outcomes of bacteremia in patients with cancer and neutropenia: Observations from two decades of epidemiological and clinical trials. *Clin. Infect. Dis.* **25**, 247–259 (1997).
31. B. Petri, M. Phillipson, P. Kubes, The physiology of leukocyte recruitment: An in vivo perspective. *J. Immunol.* **180**, 6439–6446 (2008).
32. C. M. Doerschuk, Mechanisms of leukocyte sequestration in inflamed lungs. *Microcirculation* **8**, 71–88 (2001).
33. H. Kubo, N. A. Doyle, L. Graham, S. D. Bhagwan, W. M. Quinlan, C. M. Doerschuk, L- and P-selectin and CD11/CD18 in intracapillary neutrophil sequestration in rabbit lungs. *Am. J. Respir. Crit. Care Med.* **159**, 267–274 (1999).
34. J. P. Mizgerd, B. B. Meek, G. J. Kutkoski, D. C. Bullard, A. L. Beaudet, C. M. Doerschuk, Selectins and neutrophil traffic: Margination and *Streptococcus pneumoniae*-induced emigration in murine lungs. *J. Exp. Med.* **184**, 639–645 (1996).
35. M. J. Hickey, C. L. V. Westhorpe, Imaging inflammatory leukocyte recruitment in kidney, lung and liver—Challenges to the multi-step paradigm. *Immunol. Cell Biol.* **91**, 281–289 (2013).
36. C. M. Doerschuk, The role of CD18-mediated adhesion in neutrophil sequestration induced by infusion of activated plasma in rabbits. *Am. J. Respir. Cell Mol. Biol.* **7**, 140–148 (1992).
37. G. P. Downey, G. S. Worthen, P. M. Henson, D. M. Hyde, Neutrophil sequestration and migration in localized pulmonary inflammation: Capillary localization and migration across the interalveolar septum. *Am. Rev. Respir. Dis.* **147**, 168–176 (1993).
38. G. S. Worthen, B. Schwab III, E. L. Elson, G. P. Downey, Mechanics of stimulated neutrophils: Cell stiffening induces retention in capillaries. *Science* **245**, 183–186 (1989).
39. C. M. Doerschuk, R. K. Winn, H. O. Coxson, J. M. Harlan, CD18-dependent and -independent mechanisms of neutrophil emigration in the pulmonary and systemic microcirculation of rabbits. *J. Immunol.* **144**, 2327–2333 (1990).
40. A. R. Burns, C. M. Doerschuk, Quantitation of L-selectin and CD18 expression on rabbit neutrophils during CD18-independent and CD18-dependent emigration in the lung. *J. Immunol.* **153**, 3177–3188 (1994).
41. C. M. Doerschuk, S. Tasaka, Q. Wang, CD11/CD18-dependent and -independent neutrophil emigration in the lungs: How do neutrophils know which route to take? *Am. J. Respir. Cell Mol. Biol.* **23**, 133–136 (2000).
42. D. Kreisel, R. G. Nava, W. Li, B. H. Zinselmeyer, B. Wang, J. Lai, R. Pless, A. E. Gelman, A. S. Krupnick, M. J. Miller, In vivo two-photon imaging reveals monocyte-dependent neutrophil extravasation during pulmonary inflammation. *Proc. Natl. Acad. Sci. U.S.A.* **107**, 18073–18078 (2010).
43. K. E. Barletta, R. E. Cagnina, K. L. Wallace, S. I. Ramos, B. Mehrad, J. Linden, Leukocyte compartments in the mouse lung: Distinguishing between marginated, interstitial, and alveolar cells in response to injury. *J. Immunol. Methods* **375**, 100–110 (2012).
44. B. V. Patel, K. C. Tatham, M. R. Wilson, K. P. O'Dea, M. Takata, In vivo compartmental analysis of leukocytes in mouse lungs. *Am. J. Physiol. Lung Cell. Mol. Physiol.* **309**, L639–L652 (2015).
45. S. C. Erzurum, G. P. Downey, D. E. Doherty, B. Schwab III, E. L. Elson, G. S. Worthen, Mechanisms of lipopolysaccharide-induced neutrophil retention. Relative contributions of adhesive and cellular mechanical properties. *J. Immunol.* **149**, 154–162 (1992).
46. B. G. Yipp, G. Andonegui, C. J. Howlett, S. M. Robbins, T. Hartung, M. Ho, P. Kubes, Profound differences in leukocyte-endothelial cell responses to lipopolysaccharide versus lipoteichoic acid. *J. Immunol.* **168**, 4650–4658 (2002).
47. M. B. Lawrence, L. V. McIntire, S. G. Eskin, Effect of flow on polymorphonuclear leukocyte/endothelial cell adhesion. *Blood* **70**, 1284–1290 (1987).
48. M. B. Lawrence, C. W. Smith, S. G. Eskin, L. V. McIntire, Effect of venous shear stress on CD18-mediated neutrophil adhesion to cultured endothelium. *Blood* **75**, 227–237 (1990).
49. M. Phillipson, B. Heit, S. A. Parsons, B. Petri, S. C. Mullaly, P. Colarusso, R. M. Gower, G. Neely, S. I. Simon, P. Kubes, Vav1 is essential for mechanotactic crawling and migration of neutrophils out of the inflamed microvasculature. *J. Immunol.* **182**, 6870–6878 (2009).
50. M. Phillipson, B. Heit, P. Colarusso, L. Liu, C. M. Ballantyne, P. Kubes, Intraluminal crawling of neutrophils to emigration sites: A molecularly distinct process from adhesion in the recruitment cascade. *J. Exp. Med.* **203**, 2569–2575 (2006).
51. G. B. Menezes, W.-Y. Lee, H. Zhou, C. C. M. Waterhouse, D. C. Cara, P. Kubes, Selective down-regulation of neutrophil Mac-1 in endotoxemic hepatic microcirculation via IL-10. *J. Immunol.* **183**, 7557–7568 (2009).
52. N. Kayagaki, M. T. Wong, I. B. Stowe, S. R. Ramani, L. C. Gonzalez, S. Akashi-Takamura, K. Miyake, J. Zhang, W. P. Lee, A. Muszyński, L. S. Forsberg, R. W. Carlson, V. M. Dixit, Noncanonical inflammasome activation by intracellular LPS independent of TLR4. *Science* **341**, 1246–1249 (2013).
53. J. A. Hagar, D. A. Powell, Y. Aachoui, R. K. Ernst, E. A. Miao, Cytoplasmic LPS activates caspase-11: Implications in TLR4-independent endotoxic shock. *Science* **341**, 1250–1253 (2013).
54. L. Liu, K. D. Puri, J. M. Penninger, P. Kubes, Leukocyte PI3Kγ and PI3Kδ have temporally distinct roles for leukocyte recruitment in vivo. *Blood* **110**, 1191–1198 (2007).
55. B. Heit, S. Tavener, E. Raharjo, P. Kubes, An intracellular signaling hierarchy determines direction of migration in opposing chemotactic gradients. *J. Cell Biol.* **159**, 91–102 (2002).
56. B. Heit, P. Colarusso, P. Kubes, Fundamentally different roles for LFA-1, Mac-1 and α_4-integrin in neutrophil chemotaxis. *J. Cell Sci.* **118**, 5205–5220 (2005).
57. W. D. Bradley, A. J. Koleske, Regulation of cell migration and morphogenesis by Abl-family kinases: Emerging mechanisms and physiological contexts. *J. Cell Sci.* **122**, 3441–3454 (2009).
58. S. Backert, S. M. Feller, S. Wessler, Emerging roles of Abl family tyrosine kinases in microbial pathogenesis. *Trends Biochem. Sci.* **33**, 80–90 (2008).
59. B. Heit, L. Liu, P. Colarusso, K. D. Puri, P. Kubes, PI3K accelerates, but is not required for, neutrophil chemotaxis to fMLP. *J. Cell Sci.* **121**, 205–214 (2008).
60. B. Heit, S. M. Robbins, C. M. Downey, Z. Guan, P. Colarusso, B. J. Miller, F. R. Jirik, P. Kubes, PTEN functions to 'prioritize' chemotactic cues and prevent 'distraction' in migrating neutrophils. *Nat. Immunol.* **9**, 743–752 (2008).
61. W. Ye, Z. Jiang, X. Lu, X. Ren, M. Deng, S. Lin, Y. Xiao, S. Lin, S. Wang, B. Li, Y. Zheng, P. Lai, J. Weng, D. Wu, Y. Ma, X. Chen, Z. Wen, Y. Chen, X. Feng, Y. Li, P. Liu, X. Du, D. Pei, Y. Yao, B. Xu, K. Ding, P. Li, GZD824 suppresses the growth of human B cell precursor acute lymphoblastic leukemia cells by inhibiting the SRC kinase and PI3K/AKT pathways. *Oncotarget* 10.18632/oncotarget.10881 (2016).
62. X. Ren, X. Pan, Z. Zhang, D. Wang, X. Lu, Y. Li, D. Wen, H. Long, J. Luo, Y. Feng, X. Zhuang, F. Zhang, J. Liu, F. Leng, X. Lang, Y. Bai, M. She, Z. Tu, J. Pan, K. Ding, Identification of GZD824 as an orally bioavailable inhibitor that targets phosphorylated and nonphosphorylated breakpoint cluster region–Abelson (Bcr-Abl) kinase and overcomes clinically acquired mutation-induced resistance against imatinib. *J. Med. Chem.* **56**, 879–894 (2013).
63. S. Kumar, J. Xu, C. Perkins, F. Guo, S. Snapper, F. D. Finkelman, Y. Zheng, M.-D. Filippi, Cdc42 regulates neutrophil migration via crosstalk between WASp, CD11b, and microtubules. *Blood* **120**, 3563–3574 (2012).
64. S. R. Clark, A. C. Ma, S. A. Tavener, B. McDonald, Z. Goodarzi, M. M. Kelly, K. D. Patel, S. Chakrabarti, E. McAvoy, G. D. Sinclair, E. M. Keys, E. Allen-Vercoe, R. Devinney, C. J. Doig, F. H. Y. Green, P. Kubes, Platelet TLR4 activates neutrophil extracellular traps to ensnare bacteria in septic blood. *Nat. Med.* **13**, 463–469 (2007).
65. J. D. Brain, R. M. Molina, M. M. DeCamp, A. E. Warner, Pulmonary intravascular macrophages: Their contribution to the mononuclear phagocyte system in 13 species. *Am. J. Physiol.* **276**, L146–L154 (1999).
66. D. Schneberger, K. Aharonson-Raz, B. Singh, Pulmonary intravascular macrophages and lung health: What are we missing? *Am. J. Physiol. Lung Cell. Mol. Physiol.* **302**, L498–L503 (2012).
67. A. F. Suffredini, R. J. Noveck, Human endotoxin administration as an experimental model in drug development. *Clin. Pharmacol. Ther.* **96**, 418–422 (2014).
68. M. Lynn, D. P. Rossignol, J. L. Wheeler, R. J. Kao, C. A. Perdomo, R. Noveck, R. Vargas, T. D'Angelo, S. Gotzkowsky, F. G. McMahon, Blocking of responses to endotoxin by E5564 in healthy volunteers with experimental endotoxemia. *J. Infect. Dis.* **187**, 631–639 (2003).
69. S. Copeland, H. S. Warren, S. F. Lowry, S. E. Calvano, D. Remick; Inflammation and the Host Response to Injury Investigators, Acute inflammatory response to endotoxin in mice and humans. *Clin. Diagn. Lab. Immunol.* **12**, 60–67 (2005).
70. M. Wilson, R. Blum, P. Dandona, S. Mousa, Effects in humans of intravenously administered endotoxin on soluble cell-adhesion molecule and inflammatory markers: A model of human diseases. *Clin. Exp. Pharmacol. Physiol.* **28**, 376–380 (2001).
71. K. Futosi, T. Németh, R. Pick, T. Vántus, B. Walzog, A. Mócsai, Dasatinib inhibits proinflammatory functions of mature human neutrophils. *Blood* **119**, 4981–4991 (2012).
72. H. Tong, B. Zhao, H. Shi, X. Ba, X. Wang, Y. Jiang, X. Zeng, c-Abl tyrosine kinase plays a critical role in β2 integrin-dependent neutrophil migration by regulating Vav1 activity. *J. Leukoc. Biol.* **93**, 611–622 (2013).

73. L. Cui, C. Chen, T. Xu, J. Zhang, X. Shang, J. Luo, L. Chen, X. Ba, X. Zeng, c-Abl kinase is required for β_2 integrin-mediated neutrophil adhesion. *J. Immunol.* **182**, 3233–3242 (2009).
74. A. Mócsai, M. Zhou, F. Meng, V. L. Tybulewicz, C. A. Lowell, Syk is required for integrin signaling in neutrophils. *Immunity* **16**, 547–558 (2002).
75. F. Meissner, R. A. Scheltema, H.-J. Mollenkopf, M. Mann, Direct proteomic quantification of the secretome of activated immune cells. *Science* **340**, 475–478 (2013).
76. B. McDonald, P. Kubes, Neutrophils and intravascular immunity in the liver during infection and sterile inflammation. *Toxicol. Pathol.* **40**, 157–165 (2012).
77. C. M. Doerschuk, M. F. Allard, B. A. Martin, A. MacKenzie, A. P. Autor, J. C. Hogg, Marginated pool of neutrophils in rabbit lungs. *J. Appl. Physiol.* **63**, 1806–1815 (1987).
78. W. M. Kuebler, A. E. Goetz, The marginated pool. *Eur. Surg. Res.* **34**, 92–100 (2002).
79. C. L. Abram, C. A. Lowell, The ins and outs of leukocyte integrin signaling. *Annu. Rev. Immunol.* **27**, 339–362 (2009).
80. D. C. Anderson, F. C. Schmalsteig, M. J. Finegold, B. J. Hughes, R. Rothlein, L. J. Miller, S. Kohl, M. E. Tosi, R. L. Jacobs, T. C. Waldrop, A. S. Goldman, W. T. Shearer, T. A. Springer, The severe and moderate phenotypes of heritable Mac-1, LFA-1 deficiency: Their quantitative definition and relation to leukocyte dysfunction and clinical features. *J. Infect. Dis.* **152**, 668–689 (1985).
81. H. Zhang, U. Y. Schaff, C. E. Green, H. Chen, M. R. Sarantos, Y. Hu, D. Wara, S. I. Simon, C. A. Lowell, Impaired integrin-dependent function in Wiskott-Aldrich syndrome protein-deficient murine and human neutrophils. *Immunity* **25**, 285–295 (2006).
82. E. van de Vijver, A. T. J. Tool, Ö. Sanal, M. Çetin, S. Ünal, S. Aytac, K. Seeger, D. Pagliara, S. Rutella, T. K. van den Berg, T. W. Kuijpers, Kindlin-3–independent adhesion of neutrophils from patients with leukocyte adhesion deficiency type III. *J. Allergy Clin. Immunol.* **133**, 1215–1218.e3 (2014).
83. M. Moser, M. Bauer, S. Schmid, R. Ruppert, S. Schmidt, M. Sixt, H.-V. Wang, M. Sperandio, R. Fässler, Kindlin-3 is required for β2 integrin-mediated leukocyte adhesion to endothelial cells. *Nat. Med.* **15**, 300–305 (2009).
84. T. W. Kuijpers, E. van de Vijver, M. A. J. Weterman, M. de Boer, A. T. J. Tool, T. K. van den Berg, M. Moser, M. E. Jakobs, K. Seeger, Ö. Sanal, S. Ünal, M. Çetin, D. Roos, A. J. Verhoeven, F. Baas, LAD-1/variant syndrome is caused by mutations in *FERMT3*. *Blood* **113**, 4740–4746 (2009).
85. J. Pillay, V. M. Kamp, E. van Hoffen, T. Visser, T. Tak, J.-W. Lammers, L. H. Ulfman, L. P. Leenen, P. Pickkers, L. Koenderman, A subset of neutrophils in human systemic inflammation inhibits T cell responses through Mac-1. *J. Clin. Invest.* **122**, 327–336 (2012).
86. M. R. Looney, E. E. Thornton, D. Sen, W. J. Lamm, R. W. Glenny, M. F. Krummel, Stabilized imaging of immune surveillance in the mouse lung. *Nat. Methods* **8**, 91–96 (2011).
87. B. Johnston, T. B. Issekutz, P. Kubes, The alpha 4-integrin supports leukocyte rolling and adhesion in chronically inflamed postcapillary venules in vivo. *J. Exp. Med.* **183**, 1995–2006 (1996).
88. S. Kanwar, D. C. Bullard, M. J. Hickey, C. W. Smith, A. L. Beaudet, B. A. Wolitzky, P. Kubes, The association between α_4-integrin, P-selectin, and E-selectin in an allergic model of inflammation. *J. Exp. Med.* **185**, 1077–1087 (1997).

Acknowledgments: We thank the Mouse Phenomics Resources Laboratory, funded by the Snyder Institute, and the Flow Cytometry Core Facility at the University of Calgary. **Funding:** This study was supported by operating grants from the Canadian Institutes of Health Research (CIHR) (RS-342013) and the Department of Critical Care Medicine at the University of Calgary and by bridge funding from the University of Calgary Medical Group to B.G.Y. Infrastructure funding was provided by the Canada Foundation for Innovation John R. Evans Leaders fund with matching support from the Alberta Enterprise and Advanced Education Research Capacity Program. B.G.Y. is a tier II Canada Research Chair in Pulmonary Immunology, Inflammation and Host Defence. P.K. was supported by the CIHR Team Grant: Health Challenges in Chronic Inflammation Initiative. P.K. is a tier I Canada Research Chair Leukocyte Recruitment in inflammatory disease. L.K. was supported by a grant from the Dutch Lung Foundation (3.2.10.052). **Author contributions:** Experiments were conducted and planned by B.G.Y., J.H.K., R.L., L.D.Z., B.P., N.S., M.H., V.G.S., T.T., L.K., P.P., A.T.J.T., T.W.K., T.K.v.d.B., M.R.L., M.F.K., and P.K. The manuscript was written and revised by B.G.Y. and P.K. Statistical analysis was performed by B.G.Y., J.H.K., and A.T.J.T. Funding was provided by B.G.Y. and P.K. **Competing interests:** The authors declare that they have no competing interests.

Submitted 31 January 2017
Accepted 4 April 2017
Published 28 April 2017
10.1126/sciimmunol.aam8929

Citation: B. G. Yipp, J. H. Kim, R. Lima, L. D. Zbytnuik, B. Petri, N. Swanlund, M. Ho, V. G. Szeto, T. Tak, L. Koenderman, P. Pickkers, A. T. J. Tool, T. W. Kuijpers, T. K. van den Berg, M. R. Looney, M. F. Krummel, P. Kubes, The lung is a host defense niche for immediate neutrophil-mediated vascular protection. *Sci. Immunol.* **2**, eaam8929 (2017).

Science Immunology

The lung is a host defense niche for immediate neutrophil-mediated vascular protection

Bryan G. Yipp, Jung Hwan Kim, Ronald Lima, Lori D. Zbytnuik, Bj?rn Petri, Nick Swanlund, May Ho, Vivian G. Szeto, Tamar Tak, Leo Koenderman, Peter Pickkers, Anton T. J. Tool, Taco W. Kuijpers, Timo K. van den Berg, Mark R. Looney, Matthew F. Krummel and Paul Kubes

Sci. Immunol. **2**, eaam8929.
DOI: 10.1126/sciimmunol.aam8929

Neutrophils get their blood up

Capillaries in the lung are critical for gas exchange. Now, Yipp *et al.* report that lung capillaries also contribute to host defense against bloodstream pathogens. They found that vascular neutrophils immediately responded to the presence of endotoxin or bloodstream infection by sequestering within the capillaries but not larger venules. These neutrophils were activated through TLR4 and MyD88 signaling, polarized, and crawled throughout the endothelium, removing lung-sequestered bacteria from circulation. Thus, pulmonary capillaries form a neutrophil niche to capture blood-borne pathogens in the lung.